Critical role of pinning defects in scroll-wave breakup in active media

S. Sridhar[1], Antina Ghosh[2] and Sitabhra Sinha[1]
[1] *The Institute of Mathematical Sciences, CIT Campus, Taramani, Chennai 600113, India. and*
[2] *Van der Waals Zeeman Institute, University of Amsterdam, Valckenierstraat 67, 1018 XE Amsterdam, The Netherlands.*
(Dated: September 29, 2011)

The breakup of rotating scroll waves in three-dimensional excitable media has been linked to important biological processes. The known mechanisms for this transition almost exclusively involve the dynamics of the scroll filament, i.e., the line connecting the phase singularities. In this paper, we describe a novel defect-induced route to breakup of a scroll wave pinned by an inexcitable obstacle partially extending through the bulk of the medium. The wave is helically wound around the defect inducing sudden changes in velocity components of the wavefront at the obstacle boundary. This results in breakup far from the filament, eventually giving rise to spatiotemporal chaos. Our results suggest a potentially critical role of pinning obstacles in the onset of life-threatening disturbances of cardiac activity.

PACS numbers:

Spatiotemporal patterns such as rotating spiral waves are frequently observed in excitable media models that describe the dynamics of a wide range of physical, chemical and biological systems [1, 2]. The ubiquity of such waves in numerous natural processes makes it imperative to understand their genesis and the means by which they can be controlled. Patterns in homogeneous active media have been the subject of intense theoretical and experimental investigations for several decades [3–5]. However, most natural systems possess significant inhomogeneities and the dynamics of waves in *disordered* media has come under increasing scrutiny in recent times [6–8]. The heterogeneities considered range from partially or wholly inexcitable obstacles [8, 9], gradients of excitation or conduction properties [10] and anisotropy in the speed of propagation [11]. Most such studies have focused on two-dimensional systems and the results show unexpected complexity, such as fractal basins of attraction for different dynamical states corresponding to pinned waves, spatiotemporal chaos and complete termination of activity [12]. Nevertheless, these "planar" models do not completely describe real systems which are necessarily three-dimensional. Adding an extra dimension is equivalent to considering the thickness of the system, so that one can in principle distinguish between phenomena on the surface and that in the bulk. More importantly, three-dimensional disordered media can exhibit novel dynamical phenomena that do not appear in lower dimensions. A frequently occurring pattern of activity in such systems is the scroll wave, which is a higher dimensional generalization of the spiral wave.[Fig. 1 (a)]. It can be visualized as a set of contiguous rotating spirals whose phase singularities describe a continuous line (filament) along the rotation axis perpendicular to the plane of the spirals [13] [Fig. 1 (c)]. Scroll waves have been experimentally observed in many natural systems including chemical waves in the Belusov-Zhabotinsky reaction [14–16], patterns of aggregation during *Dictyostelium* morphogenesis [17, 18] and electrical waves in heart muscles [2]. Indeed scroll waves have been implicated in several types of arrhythmia, i.e., disturbances in the natural rhythmic activity of the heart that can be potentially fatal. Under certain conditions these three-dimensional waves can develop instabilities and break up into multiple scroll fragments. The ensuing spatiotemporally chaotic state of excitation is associated with the complete loss of coherent cardiac activity in life-threatening arrhythmia such as ventricular fibrillation [19, 20]. Therefore a deeper understanding of the mechanisms that lead to chaotic activity through breakup of scroll waves is of great practical significance.

At present almost all proposed scenarios for scroll wave breaking involve complex filament dynamics [21]. The question of whether there can be other mechanisms, especially one involving breakup far from the singularities, is of special significance when considering disordered media. This is because heterogeneities such as inexcitable obstacles can anchor rotating waves and stabilize filament dynamics preventing the usual breakup scenario. While interaction of scroll waves with inexcitable obstacles have recently been investigated [22–25], the existence of several types of disorder in the systems considered in these studies do not clearly reveal the exact mechanisms for wavebreaks that are involved. By focusing on a simplified situation of a defect with regular geometry we ask whether there can be a purely obstacle-induced breakup mechanism for scroll waves.

In this paper, we have considered an isotropic three-dimensional system with an inexcitable obstacle of uniform cross-section that does not span the entire thickness of the medium [Fig. 1 (b)]. This is motivated by the physiological observation that an inexcitable obstacle may be located deep in the bulk of heart tissue, where it cannot be detected through electrophysiological imaging of the surface [26]. We show a novel dynamical transition that can occur in such a situation which does not appear in the absence of a defect, nor in the effectively two-dimensional situation when the obstacle spans the thickness of the medium. The differential rotation pe-

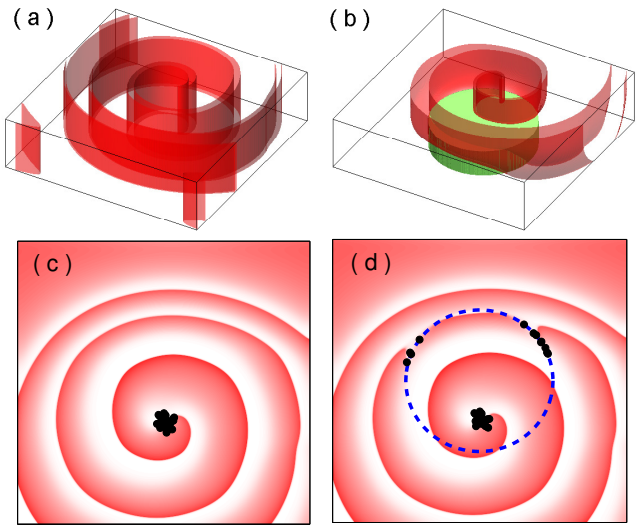

FIG. 1: Scroll waves in (a) a homogeneous medium and (b) a medium having an inexcitable cylinder-shaped obstacle that extends only partly through the bulk of the medium. (c-d) Pseudocolor images of spiral waves observed in a cross-sectional plane perpendicular to the axis of rotation, for the systems shown in (a) and (b) respectively. The black dots correspond to the intersection of the plane with the filament at different times, indicating the trajectory of the phase singularity in the plane. In (d), the plane chosen is just above the upper bounding surface of the obstacle whose circumference is indicated using broken lines. The appearance of additional black dots along the broken circle in (d) indicates a wavebreak induced by the obstacle at its boundary, far from the existing scroll filament.

riods in various sections of the wave results in a helical structure wound around the obstacle that in most cases attains a steady state after some initial transient activity. However, under certain circumstances, the wave can break near the bounding edge of the obstacle and far from the scroll wave filament [Fig. 1 (d)]. This happens when the wavefront velocity decreases sharply at the edge as a result of sudden change in its curvature. As a result, the interaction between its waveback and the succeeding wavefront may lead to a conduction block, "tearing" the latter which evolves into a pair of counter-rotating scroll waves. The process can repeat, thereby creating multiple filaments which interact with each other leading to fully developed spatiotemporal chaos. The novelty of the mechanism presented in this paper lies in the fact that the breakup does not involve the filament, unlike the previously proposed pathways for the onset of chaos in three-dimensional excitable media. It is especially relevant for disordered media as the transition to chaos is essentially defect induced because the wave is *stable* (i.e., does not break or result in the generation of additional filaments) in the absence of the inexcitable obstacle. Moreover, this is a genuine three-dimensional phenomenon that cannot be observed in lower-dimensional systems.

To simulate spatiotemporal activity in three-dimensional excitable tissue, we use models having the generic form,

$$\frac{\partial V}{\partial t} = -\frac{I_{ion}(V, g_i)}{C_m} + \nabla . D \nabla V, \qquad (1)$$

where V is the activation variable, typically, the potential difference across a cellular membrane (measured in mV), C_m (= 1 μF cm^{-2}) is the transmembrane capacitance, D represents the inhomogeneous intracellular coupling, I_{ion} (μA cm^{-2}) is the total current density through ion channels on the cellular membrane, and g_i describe the dynamics of gating variables of different ion channels. The specific functional form for I_{ion} varies for different biological systems. For the results reported here we have used the Luo-Rudy I (LR1) model that describes the ionic currents in a ventricular cell [27] with the following modifications. The maximum K^+ channel conductance G_K has been increased to 0.705 mS cm^{-2} to reduce the action potential duration (APD) making it comparable to that in the human ventricle [28]. To avoid spontaneous scroll breakup in the absence of any obstacle, the slow inward Ca^{2+} channel conductance G_{si} has been set to ≤ 0.04 mS cm^{-2} [29]. We have explicitly verified that our results are not sensitively dependent on model-specific details (e.g., description of ion channels) by observing similar effects in the simpler phenomenological model proposed by Panfilov (PV) [30].

The equations are solved using a forward-Euler scheme with time-step $\delta t = 0.01$ ms in a three-dimensional simulation domain having $L \times L \times L$ points. For most results reported here $L = 400$, although we have verified their size independence by repeating our simulations with different L (viz., upto 600). The space step used is $\delta x = 0.0225$ cm, with a standard 7-point stencil for the Laplacian describing the spatial coupling. No-flux boundary conditions are applied on the boundary planes of the simulation domain as well as along the walls of the inexcitable obstacle. The coupling D is set to zero inside the obstacle, while outside it is 0.001 cm^{2}s^{-1}. We have considered obstacles of different shapes, including cylinders and cuboids, and have not observed qualitative differences between them. Obstacles are characterized by their height L_z (beginning from the base of the simulation domain and ranging between 0 to L) and cross-sectional area (viz., πR^2 for cylinders where R is the radius and $L' \times L'$ for a cuboid). The initial scroll wave, with its filament aligned along the L_z-axis, is obtained by breaking a 3-dimensional planar wavefront. Qualitatively similar results are achieved with waves having curved filaments.

The most important result obtained from our simulations is that a sufficiently large pinning defect can promote wavebreaks in an otherwise stable rotating wave (Fig. 2). At the initial stage, when a broken wave is anchored by the obstacle, the partial extension of the latter through the bulk of the medium produces differential rotation speeds of the scroll wave along the L_z-axis. Far above the obstacle the period is closer to T_{free}, that of a free scroll wave unattached to any obstacle, while at

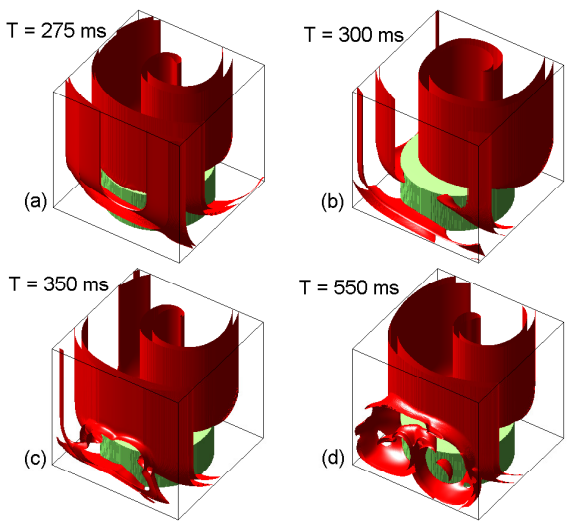

FIG. 2: Breakup of a scroll wave induced by a cylindrical obstacle ($R = 3.4$ cm, $L_z = 2.7$ cm) (a) By $T = 275$ ms after the initial wave-break, the resulting scroll wave has wound itself around the obstacle. (b) A wavefront detaches from the surface of the obstacle, at the boundary of its upper surface, by $T = 300$ ms. This broken wavefront eventually evolves into new scroll wave filaments (c-d). The period of a free (unpinned) scroll wave in this parameter regime is $T_{free} = 65.13$ ms.

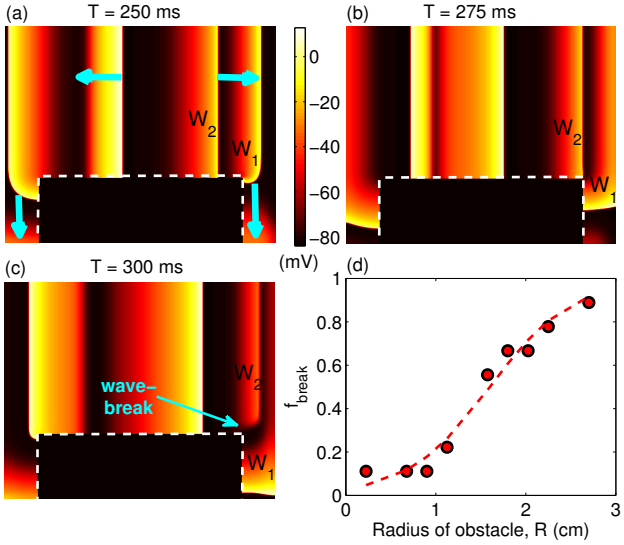

FIG. 3: (a-c)Pseudocolor plots of the transmembrane potential V for a cross-section of the system shown in Fig. 2, along a plane parallel to the L_z-axis. Boundary of the obstacle (shaded) is marked by broken lines. The arrows in (a) indicate the direction of propagation for wavefronts. The wave W_1 slows down at the boundary of the upper surface of the obstacle. As a result, the wave W_2 closely following W_1 encounters a region that has not fully recovered from its prior excitation by W_1, leading to (c) the detachment of W_2 from the surface of the obstacle and formation of a singularity. (d) The fraction of initial conditions that result in scroll wave breakup by $T = 3$ s, $f_{breakup}$, as a function of the obstacle size. The broken line is a sigmoid fit to the data.

the base of the obstacle the period $T_{pinned} \sim C/c$ is substantially slower depending upon the circumference C of the obstacle (c being the average propagation speed normal to the wavefront). This results in a helical winding of the scroll wave around the obstacle until a steady state is achieved when the rotation period becomes same across the domain [Fig. 2 (a)]. The pitch of the wound scroll wave depends on the obstacle size, with larger C resulting in a tighter winding, i.e., smaller pitch. Note that the filament of the resulting scroll wave, which stretches from the top of the obstacle to the upper boundary of the simulation domain, remains same as that of a free scroll wave (Fig. 1). When the wavefront is close to the filament it has velocity components only along the plane perpendicular to the L_z-axis. However, when the wave crosses the obstacle boundary, it develops a velocity component parallel to the L_z-axis as the front travels down the vertical sides of the obstacle. The magnitude of the change in velocity depends on the pitch of the helical winding, and hence on the circumference of the obstacle, with larger obstacles resulting in greater velocity differences. There is a corresponding change in the curvature of the wave along a plane parallel to L_z-axis. As seen in Fig. 2 (b), this sudden change in velocity components as the front crosses the edge of the obstacle upper surface may result in detachment of a succeeding wave from the obstacle surface. This is manifested as a "tear" on the wavefront surface as it breaks generating a pair of new filaments [Fig. 2 (c)]. Further evolution of the system produces more complex wave fragments as the filaments interact with each other [Fig. 2 (d)], eventually leading to spatiotemporal chaos.

To better understand the mechanism by which the pinned scroll wave breaks, we consider the cross-sectional view of the system parallel to the L_z-axis [Fig. 3 (a-c)]. Fig. 3 (a) indicates the direction of propagation as the waves move first along the upper surface and then down the vertical sides of the obstacle (shaded dark in the figures). The wave W_1 slows down as it moves past the boundary of the upper surface of the obstacle This results from the sudden change in the velocity components of the front mentioned earlier and is associated with an increased curvature of the wave [31]. Thus, the wave W_2 closely following W_1 encounters an incompletely recovered region at the edge of the obstacle [Fig. 3 (b)]. The resulting propagation block of W_2 in the direction parallel to the L_z-axis (immediately adjacent to the obstacle boundary), dislodges the wave from the surface of the obstacle and generates a singularity at the point where the scroll wave breaks [Fig. 3 (c)]. This phenomenon can be further enhanced by filament meandering that results in Doppler-effect induced changes in the propagation speed of successive waves. As previously mentioned, larger obstacles result in sharper differences in the velocity (and curvature) of the front as it crosses the obstacle, that suggests increased probability of wavebreak with increasing

C. This is indeed observed in Fig. 3 (d) supporting the mechanism outlined above.

The significance of the results reported here lies in the fact that almost all previously reported mechanisms by which scroll waves break up leading to spatiotemporal chaos necessarily involves the dynamics of the filament, e.g., negative filament tension in low excitability regime or filament twist instabilities in the presence of cardiac fiber rotation [21]. By contrast, the novel transition route to chaos described in this paper is a result of changes in the wavefront velocity components at the edge of a pinning obstacle, far from the existing filament. While there exist a few other mechanisms which can lead to scroll waves breaking, e.g., decreased cell coupling, these are not exclusively three-dimensional phenomena and are known to be involved in two-dimensional spiral wave breakup [21].

We stress that the mechanism described here has no two-dimensional analog. While wavebreaks can be created through interaction between high-frequency excitation fronts with an inexcitable obstacle in two-dimensional media [6], the corresponding situation in our three-dimensional system, where the waves encountering an obstacle originate from a scroll wave filament located *far* from the obstacle (and not pinned by it), does not result in wavebreaks. This is because, in this case, the wavefront splits and rejoins as it travels around the inexcitable obstacle without creation of any new velocity components. Therefore, unlike the pinned scroll wave considered earlier, the wavefront conduction speed is not reduced significantly.

The role played by a three-dimensional obstacle in inducing the breakup of an otherwise stable rotating wave is extremely pertinent for understanding the genesis of certain cardiac arrhythmias as an ageing heart gradually accumulates defects through increased instances of local tissue necrosis [32]. While obstacles in three-dimensional media that do not extend through the entire thickness of the system have been considered earlier, these studies focused on the depinning transition of scroll waves in the presence of drift inducing parameter gradients [22, 23]. In contrast, we show that such defects can give rise to complex dynamics including transition to chaos.

In conclusion, we have shown that the presence of an inexcitable obstacle in three-dimensional excitable media can result in scroll wave breakup far from the filament through a novel physical mechanism. The helical winding of wave around a pinning defect causes sudden changes in the velocity components of the wavefront as it crosses the boundary of the obstacle, with an associated increase in the curvature of the wave in the plane parallel to the axis of its rotation. The resulting enhanced interaction between successive waves at the bounding edge of the obstacle increases the probability of a wavefront detaching from the surface of the obstacle giving rise to new filaments. These wavebreaks can eventually lead to spatiotemporal chaos, manifested as fibrillation in the heart. Thus, our results may have consequences for understanding the critical role of defects (such as, inexcitable regions of necrotic tissue) embedded deep inside the bulk of cardiac muscle in the genesis of life-threatening arrhythmia.

This work was supported in part by IMSc Complex Systems Project (XI Plan) and IFCPAR Project 3404-4. We thank I. R. Efimov and R. Singh for helpful discussions.

[1] M. C. Cross and P. C. Hohenberg, Rev. Mod. Phys. **65**, 851 (1993).
[2] J. Keener and J. Sneyd, *Mathematical Physiology*, Springer, New York, 1998.
[3] V. S. Zykov, Biofizika **31**, 940 (1986).
[4] A. T. Winfree, Science **175**, 634 (1972).
[5] E. Meron, Physics Reports **218**, 1 (1992).
[6] A. V. Panfilov and J. P. Keener, J. Theor. Biol. **163**, 439 (1993).
[7] F. Xie, Z. Qu and A. Garfinkel, Phys. Rev. E. **58**, 6355 (1998).
[8] S. Sinha, K. M. Stein and D. J. Christini, Chaos **12**, 893 (2002); S. Sinha and D. J. Christini, Phys. Rev. E. **66**, 061903 (2002).
[9] A. Pumir *et al.*, Phys. Rev. E **81**, 010901(R) (2010).
[10] S. Sridhar, S. Sinha and A. V. Panfilov, Phys. Rev. E **82**, 051908 (2010).
[11] V. Krinsky and A. Pumir, Chaos **8**, 188 (1998).
[12] T. K. Shajahan, S. Sinha and R. Pandit, Int. J. Mod. Phys. B. **17**, 5645 (2003); T. K. Shajahan, S. Sinha and R. Pandit, Phys. Rev. E. **75**, 011929 (2007); T. K. Shajahan, A. R. Nayak and R. Pandit, PLoS One **4**, e4738 (2009);
[13] A. T. Winfree, *When Time Breaks Down*, Princeton Univ. Press, Princeton, NJ, 1987.
[14] A. T. Winfree, Science, **181**, 937 (1973).
[15] B. J. Welsh, J. Gomatam and A. E. Burgess, Nature (London) **304**, 611 (1983).
[16] V. G. Fast and A. M. Pertsov, Biophysics **35**, 489 (1990).
[17] O. Steinbock, F. Siegert, S. C. Muller and C. J. Weijer, Proc. Natl. Acad. Sci. USA **90**, 7332 (1993).
[18] C. J. Weijer, Seminars in Cell and Developmental Biology **10**, 609 (1999).
[19] R. A. Gray, A. M. Pertsov, and J. Jalife, Nature (London) 392, 75 (1998).
[20] F. X. Witkowski *et al.*, Nature (London) 392, 78 (1998).
[21] F. H. Fenton *et al.*, Chaos **12**, 852 (2002).
[22] M. Vinson, A. Pertsov and J. Jalife, Physica D **72** 119 (1993).
[23] A. Pertsov and M. Vinson, Phil. Trans. R. Soc. Lond. A **347**, 687 (1994).
[24] Z. A. Jimenez, B. Marts and O. Steinbock, Phys. Rev. Lett. **102**, 244101 (2009).
[25] R. Majumder, A. R. Nayak and R. Pandit, PLoS One **6** e18052 (2011).
[26] N. S. Peters *et al.*, Circulation **95**, 988 (1997); N. S.

Peters *et al.*, Circ. Res. **82**, 279 (1998).
[27] C. H. Luo and Y. Rudy, Circ. Res **68**, 1501 (1991).
[28] K.H.W.J. ten Tusscher and A. V. Panfilov, Am. J. Physiol. Heart Circ. Physiol. **284**, H542 (2003).
[29] We have explicitly verified that the scroll wave does not break up in absence of any obstacle by evolving the system for long durations ($> 10^4$ ms).
[30] A. V. Panfilov, Chaos **8**, 57 (1998).
[31] A. S. Mikhailov, V. A. Davydov and V. S. Zykov, Physica D **70**, 1 (1994).
[32] D. P. Zipes and J. Jalife, *Cardiac Electrophysiology: From Cell to Bedside*, Saunders, Philadelphia, 2004.